Effect of Non-ionic Surfactants on the Adsorption of Polycyclic Aromatic Compounds at Water/Oil interface: A Molecular Simulation Study

Xiaoyu Sun[†], Hongbo Zeng[,†], Tian Tang[*,‡]*

[†]Department of Chemical and Materials Engineering, University of Alberta, Edmonton, AB T6G 1H9, Canada

[‡]Department of Mechanical Engineering, University of Alberta, Edmonton, AB T6G 1H9, Canada

** Corresponding authors:*

E-mail: hongbo.zeng@ualberta.ca (H.Z.); Phone: +1-780-492-1044;

E-mail: tian.tang@ualberta.ca (T.T.); Phone: +1-780-492-5467.

Abstract

Hypothesis

Molecular simulations can provide unique insights into the adsorption and intermolecular interactions of polycyclic aromatic compounds (PACs) and non-ionic surfactants at water/oil interface.

Methods

Molecular dynamic simulations were performed to study the adsorption of PACs at water/oil interface, and the effect of adding non-ionic surfactants. PAC architecture, solvent type, structure and concentration of non-ionic surfactants were varied to address the complex interplay between PAC-surfactant interaction, PAC solubility, and structure-dependent PAC aggregation.

Findings

PAC with multiple cores (PacM) partially adsorbed on the interface, in the form of small and loosely structured aggregates. Adding non-ionic surfactant Brij-93 induced desorption of PacM at both water/toluene and water/heptane interfaces. Another non-ionic surfactant, $(EO)_5(PO)_{10}(EO)_5$, also reduced the adsorption of PacM at water/toluene interface but enhanced their adsorption at water/heptane interface. PACs with a single large core strongly adsorbed on both interfaces, forming compact aggregated structures. Adding the two types of non-ionic surfactants did not induce desorption. This work identified two opposite roles of non-ionic surfactants in the adsorption of PACs, namely competition and co-adsorption, and provided useful insights into how the roles of non-ionic surfactants might be affected by their concentration, as well as the solubility and interfacial behaviors of the PACs.

Keywords: water/oil interface; non-ionic surfactant; polycyclic aromatic compound; adsorption; simulation.

1. Introduction

Understanding the adsorption of surface-active components at liquid/liquid interfaces is essential for many colloidal processes and industrial applications. [1,2] Transportation of surface-active components from one liquid phase to another plays important roles in extraction and separation processes, which involves the important step of interfacial adsorption. [3–5] Interfacially adsorbed molecules with functional groups could form well-organized aggregates, which are suitable as catalysts, biosensors, drug delivery agent, etc. [6–8] Emulsification occurs when the interface between two immiscible liquids (e.g., water and oil) is stabilized by the adsorption of surface-active components. [9] Stable emulsions are desirable in applications such as food, pharmaceutical, and cosmetic industries. [10–14] On the other hand, water/oil emulsification is highly undesirable in petroleum industry because it causes difficulty in oil/water separation, increases the corrosion of equipment and pipelines, and reduces the transportation efficiency. [15–17]

The adsorption of polycyclic aromatic compounds (PACs) on the water/oil interface has attracted wide attention in environmental [18–23] and industrial research [24–27]. PACs, naturally present in fossil fuel, contain polycyclic aromatic hydrocarbon (PAH) core(s) and aliphatic chains, which generally have functional groups with heteroatoms such as sulfur, oxygen and nitrogen. These molecules exhibit amphiphilic and surface-active features and can be adsorbed at the water/oil interface. Consequently, they become organic contaminates and accumulate in soil and ocean as oil spills [18–23]. For example, Zhu et al. [23] studied the co-existence of PAH (anthracene) and cyclodextrin on water/chloroform interface, as a means to extract PAH pollutants from the oil phase. The cyclodextrin was found to be able to transport spontaneously from water phase to the water/oil interface, indicated by the negative free energy change. The PAH preferred

to be included into the cyclodextrin aggregates on the water/oil interface instead of in bulk oil. The same authors [28] reported the co-aggregation of humic acid and PACs at water/toluene interface, and suggested that the co-aggregation increased the retainment of the oil contaminants in aqueous environments. [28] Various non-ionic surfactants have been explored for remediation of PACs from contaminated soil or water [20,21], as they increased the dissolution rate and solubility of PACs in the aqueous phase and promoted the efficiency of groundwater flushing [29].

Beside pollutant treatment, non-ionic surfactants was frequently applied as destabilisers for unwanted emulsions stabilized by PACs. [30] Water and oil emulsification was commonly attributed to the formation of a stable and rigid film of surface-active components at the water/oil interface, [15–17] among which the PACs were a main contributor. The water and oil emulsions include water-in-oil (W-O), oil-in-water (O-W), and more complex cases like water-in-oil-in-water (W-O-W) emulsions, where the W-O emulsion is the predominant type. To break up the W-O emulsion, various non-ionic surfactants have been used for chemical demulsification. [30–32] The experiments of Li et al. [33] studied the demulsification of water-in-aging-crude-oil emulsion by novel tannic acid phenol-amine polyether with multiple branches. They proposed that the hydrophilic branches entered the interior of the water droplets while the hydrophobic parts stayed on the surface, which had the strong interaction with the PACs in the protective film and could partially break up the film. [33] PEO-PPO copolymers, a group of non-ionic surfactants, have been commonly synthesized and used for W-O demulsification processes. [34–37] Their demulsification performance, i.e. the water removal efficiency, was affected by many factors such as the number of copolymer branches [34], molecular weight, PPO/PEO ratio [36], and concentration [35]. For example, Cendejas et al. [35] attributed the optimal water separation from water-in-crude-oil emulsion at certain concentration of PEO-PPO copolymer to the saturation of

polymeric chains at the water/oil interface. The desorption mechanism of PACs from water/xylene interface by PEO-PPO co-polymer, as well as Brij-93, was investigated by Pradilla et al. [38,39] They added the non-ionic surfactants to the water/xylene interface with already adsorbed PACs and carried out interfacial tension measurement to assess the desorption of PACs at the interface. [38,39] The composition of non-ionic surfactants and PACs on the mixed interface was calculated using the Langmuir equation of state. [38,39] At low concentration of non-ionic surfactants (10 ppm for Brij-93 and 0.5 ppm for PPO-PEO co-polymers), interaction between non-ionic surfactants and PACs was detected on the interface, while the PAC desorption was partial or negligible. [38] At 2500 ppm Brij-93 and 100 ppm PPO-PEO co-polymers, the PACs were completely replaced from the interface and had no interaction with the surfactants. [38] The authors proposed that the desorption of PACs was initiated by the interaction between the non-ionic surfactants and PACs, followed by the formation of complex structure between them, and finally the displacement of PACs by the surfactants. [38] While experimental studies frequently attributed the demulsification mechanisms to the interactions of PACs with non-ionic surfactants on the interface, molecular-level evidence of the interactions was difficult to obtain by experimental approach alone.

Theoretical investigations, by the means of molecular simulations, have provided direct observations on the interfacial adsorption and interaction of PACs and surfactants, and contributed to the understanding of demulsification mechanisms. Many studies have been carried out on water/oil interface with solely PACs [40–42] or non-ionic surfactants [2,43]; few works simulated the co-existence of PACs and surfactants. For example, molecular dynamics (MD) simulation was carried out by Niu et al. [44] on water/xylene interface with adsorbed C5Pe, a model PAC molecule, by adding a PEO-PPO triblock copolymer. The copolymer was found to be more surface active

than C5Pe and could form stronger hydrogen bonding with water. [44] The adsorbed copolymers replaced C5Pe molecules and broke up the rigid C5Pe film at the water-xylene interface, which would ultimately assist the coalescence of water droplets. [44]

In spite of experimental and theoretical approaches to understand the demulsification mechanism by non-ionic surfactants, molecular level investigation on the intermolecular interactions between PACs and non-ionic surfactants on the water/oil interface is still in demand. Especially, there is a lack of systematic theoretical investigation on the factors that affect the demulsification process. For example, various non-ionic surfactants have been applied as destabilizers and the demulsification mechanisms can vary greatly. [30,45,46] While many reports studied the popular PEO-PPO copolymers, other non-ionic surfactants have been much less discussed, such as the Brij group which has been compared with PEO-PPO copolymers in experiments [38,39]. Additionally, PACs have complex structures that yield different surface-activity [47]. For example, it was suggested that PACs with moderate polarity could be adsorbed readily at the water/oil interface to stabilize the emulsion, while the stability was reduced when PACs with low or high polarity were adsorbed. [48] Mixtures of PACs were generally used in experimental studies, and there is a lack of comparison between different PAC structures in the demulsification by non-ionic surfactants. Also, the oil phase could be represented by various organic solvents, among which the aromatic solvent (toluene) and aliphatic solvent (heptane) were commonly compared. The emulsion was generally less stable with PACs on water/heptane interface than on water/toluene interface, which was attributed to the change in the aggregation state of PACs on the interface. [49] It remains unclear how the solvent type would affect the demulsification by non-ionic surfactants at the molecular level.

This work aims to use MD simulations to provide a comprehensive understanding on the effect of non-ionic surfactant on the adsorption of PACs at water/oil interface, by considering several factors, such as PAC architecture, solvent types, structures and concentration of non-ionic surfactants. To achieve this objective, model PAC molecules with a single polyaromatic (PA) core and multiple PA cores were simulated. The effect of solvent types was studied by representing the oil phase with two different organic solvents: one aromatic (toluene) and the other aliphatic (heptane). A model PEO-PPO copolymer, $(EO)_5(PO)_{10}(EO)_5$, was introduced to examine its capability of desorbing the PACs from the oil/water interface. Comparison was made with another widely used non-ionic surfactant from Brij family, Brij-93 [38,39]. Finally, each of the two non-ionic surfactants was applied into the organic phase at two concentrations. The interactions between PACs, non-ionic surfactants and interface were analyzed at the molecular level, to provide mechanistic insights into the stabilization and destabilization of water/oil interfaces.

2. Methods

2.1 Molecular models

Two PAC models were used in this work, one of which had multiple PA cores and the other had a single PA core. The PAC with multiple PA cores, referred to as "PacM", was hypothesized based on C5-insoluble asphaltenes [50,51] from Athabasca bitumen, as shown in Fig. 1a. PacM has a molecular weight (MW) of 1303 g/mol and chemical composition as: C 81.12; H 7.97; N 1.07; O 2.46; S 7.38 (%wt.). There are six heteroatoms including 2 oxygen atoms, 3 sulfur atoms and 1 nitrogen atom. The other PAC with a single PA core, Violenthrane-79 (VO-79), has been extensively studied [52,53] and is referred to as "PacS" in this work. PacS has a chemical formula of $C_{50}H_{48}O_4$ with MW of 712 g/mol, as shown in Fig. 1b. One of the non-ionic surfactants used

was polyethylene glycol oleyl ether $C_{22}H_{44}O_3$ (Brij-93) with average MW of 357 g/mol (Fig. 1c), which is referred to as NisB in this work. The other model non-ionic surfactant simulated was $(EO)_5(PO)_{10}(EO)_5$ (referred to as NisP, MW: 1039 g/mol), a typical triblock copolymer with equal number of EO and PO branches as shown in Fig. 1d.

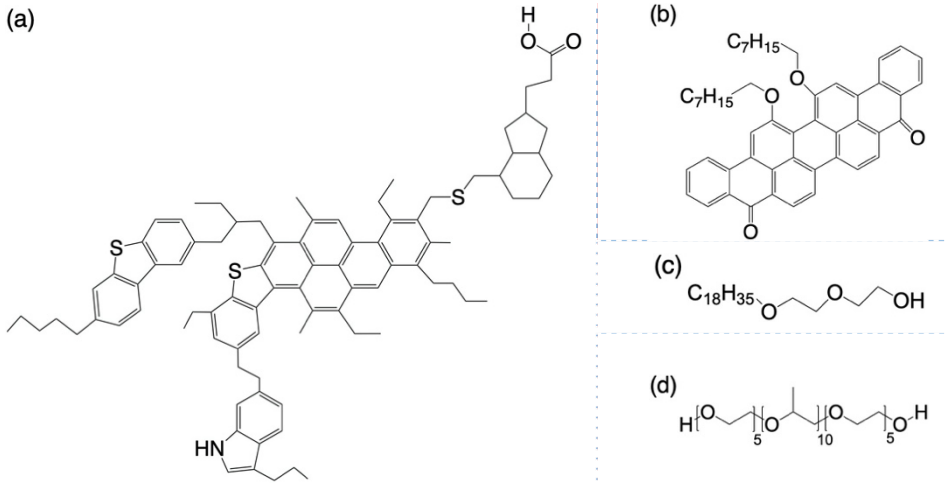

Figure 1. Molecular structures of (a) PacM, (b) PacS, (c) NisB, and (d) NisP.

Initial chemical structure of PacM was drawn in ChemDraw Prime 16.0. Geometry optimization of PacM was first performed by density functional theory (DFT) calculation at B3LYP/6-31G + (d,p) level [54]. The obtained geometry was further optimized using Automated Topology Builder (ATB) [55], in order to generate force field parameters compatible with the GROMOS96 parameter sets [56]. The partial atomic charges were determined from the electrostatic potential calculated at B3LYP /6-31G + (d,p) level, with the CHELPG (CHarges from ELectrostatic Potentials using a Grid based method) [57] method. The partial charges were then manually mapped to the topology generated from ATB. The parameters for NisB and NisP were obtained following the same procedure. All quantum-chemical calculations were carried out using the Gaussian 16 software package [58]. Models for PacS, toluene and heptane were adopted from previous publications in our group [59]; the parameterization steps were identical except the use

of def2-SV(P) basis set. Single point charge (SPC) model was used for water molecules, which has been extensively applied and validated. [60] The densities of pure PACs (PacM, PacS) and non-ionic surfactants (NisB, NisP) were further validated against the experimental data in the literature, as explained in Supporting Information (SI) section SI1.

2.2 Simulated systems

A total of 20 systems were simulated, with details given in Table 1. The name of each system starts with a letter of T or H, corresponding to toluene and heptane being the organic solvent (oil phase), respectively. The second letter indicates the type of PAC molecules: M for PacM and S for PacS. The non-ionic surfactants, NisB and NisP, are labeled as B and P after the type of PACs. The label is finally followed by “low” or “high”, which corresponds to relatively low and high concentrations of the surfactants. Sys. 1, 6, 11 and 16 do not contain any non-ionic surfactants and are used as control systems. Each system contained 32 PAC molecules. In the system with PacM and a low concentration of NisB, 32 NisB molecules were introduced, leading to the same molar concentration between NisB and PacM. A high concentration of NisB corresponded to 124 NisB molecules, which had a mass concentration comparable to PacM. The number of NisP molecules were also decided to render comparable molar (low concentration) or mass (high concentration) ratios between NisP and PacM. The same number of non-ionic surfactants were added to systems containing PacS.

Table 1. Details of simulated systems. (sys. 1 TM, sys. 6 HM, sys. 11 TS, and sys. HS are control systems without adding non-ionic surfactants)

Sys.	Name	Solvent	no. of PacM	no. of PacS	no. of NisB	no. of NisP	Molar ratio (PAC/NIS)	Mass ratio (PAC/NIS)
1	TM	Toluene	32	-	-	-	-	
2	TM-B-low	Toluene	32	-	32	-	1:1	1:0.27
3	TM-B-high	Toluene	32	-	128	-	1:4	1:1.1
4	TM-P-low	Toluene	32	-	-	24	1:0.75	1:0.6
5	TM-P-high	Toluene	32	-	-	48	1:1.5	1:1.2
6	HM	Heptane	32	-	-	-		
7	HM-B-low	Heptane	32	-	32	-	1:1	1:0.27
8	HM-B-high	Heptane	32	-	128	-	1:4	1:1.1
9	HM-P-low	Heptane	32	-	-	24	1:0.75	1:0.6
10	HM-P-high	Heptane	32	-	-	48	1:1.5	1:1.2
11	TS	Toluene	-	32	-	-		
12	TS-B-low	Toluene	-	32	32	-	1:1	1:0.5
13	TS-B-high	Toluene	-	32	128	-	1:4	1:2
14	TS-P-low	Toluene	-	32	-	24	1:0.75	1:1.1
15	TS-P-high	Toluene	-	32	-	48	1:1.5	1:2.2
16	HS	Heptane	-	32	-	-		
17	HS-B-low	Heptane	-	32	32	-	1:1	1:0.5
18	HS-B-high	Heptane	-	32	128	-	1:4	1:2
19	HS-P-low	Heptane	-	32	-	24	1:0.75	1:1.1
20	HS-P-high	Heptane	-	32	-	48	1:1.5	1:2.2

2.3 Simulation details

To construct the initial configuration for the control systems, a box with dimension of 12×12×12 nm^3 was filled with water [61]. As shown in Fig. 2a, the box was then extended in z direction to 24 nm, where the PacM/S were aligned in an array of 4×4×2 next to the water box. The extended box containing PacM/S molecules was then filled by organic solvent (toluene or heptane), which formed the initial configuration for the control systems, as shown in Fig. 2b. After equilibration, the final configuration of PacM/S adsorbed at the interface was obtained, as shown in Fig. 2c. This was used to construct the initial configuration for systems with non-ionic surfactants (NisB/P) by the following steps in Fig. 2: removing the solvent (Fig. 2d), adding NisB/P (Fig. 2e), and filling the right side of the simulation box with organic solvent (Fig. 2f).

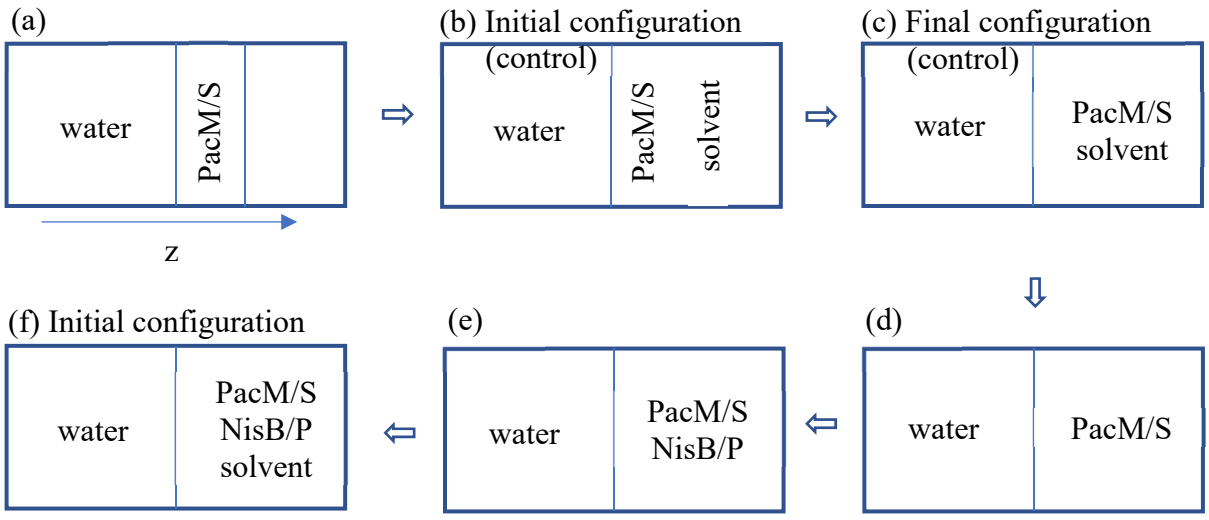

Figure 2. Schematic representation of the construction of initial configurations.

All simulations were performed by using GROMACS package [62–64] (version 5.0.7) with GROMOS 96 force field parameter set 53A6 [65]. Each simulation underwent an energy minimization process for static structure optimization. Then, a short *NVT* simulation was carried out with position-restraints on the non-hydrogen atoms of PAC, using a harmonic potential of force constant 1000 kJ/(mol·nm^2). The restraint was removed, and full dynamics simulation was carried out in NpT ensemble at 300 K and 1 bar. The pressure was controlled by isotropic Parrinello-Rahman barostat with time constant τ_p of 1 ps and compressibility of 4.5×10^{-5} bar^{-1}. The temperature was controlled by velocity rescaling thermostat with time constant τ_T of 0.1 ps. For each simulation, LINCS [66] algorithm and Particle Mesh Ewald method for full electrostatics [67] were applied. The cut-off for non-bonded (van der Waals and electrostatic) interactions was set to 1.4 nm. Periodic boundary conditions in all three directions were applied. All simulations had a time step of 2 fs, and the total simulation time was 60 ns for each system, except sys. 1 which was simulated for 120 ns.

3. Results and discussion

3.1 Adsorption and desorption of PacM

Control systems with PacM on water/toluene (sys. 1) and water/heptane (sys. 6) interfaces were simulated before adding the non-ionic surfactants. Density profiles of water, organic solvent and PacM are shown in Figs. 3a and 3b, respectively for sys. 1 and 6, with final configurations of the systems above the plot. The density profiles were averaged over the last 5 ns when the adsorption of PACs was stable, as shown in SI section SI2. Compared with Fig. 2, the simulation boxes in Fig. 3 were each translated by 6 nm along -z direction, in order to better show the interfaces between water and organic solvent. For the rest of this paper and in the SI, the same translation was applied to all figures containing snapshots and density profiles. Due to the periodic boundary condition, each system had two interfaces, obtained from the intersection of the density profiles for water and toluene (or heptane), which were marked by blue arrows. The left interface was located at z = ~6 nm, referred to as interface-L. The right interface, referred to as interface-R, was located around 18 nm for sys. 1 and 11, and around 20 nm for sys. 6 and sys. 16. The density profile of PacM in each system had two peaks each near one of the interfaces, indicating the adsorption of PacM molecules. Also shown in Fig. 3a, PacM had non-zero density in the bulk toluene phase, consistent with the snapshot where many PacM molecules were dispersed in bulk toluene. On the contrary, in Fig. 3b the density of PacM was close to zero in bulk heptane, and the vast majority of the PacM molecules were located close to the interfaces.

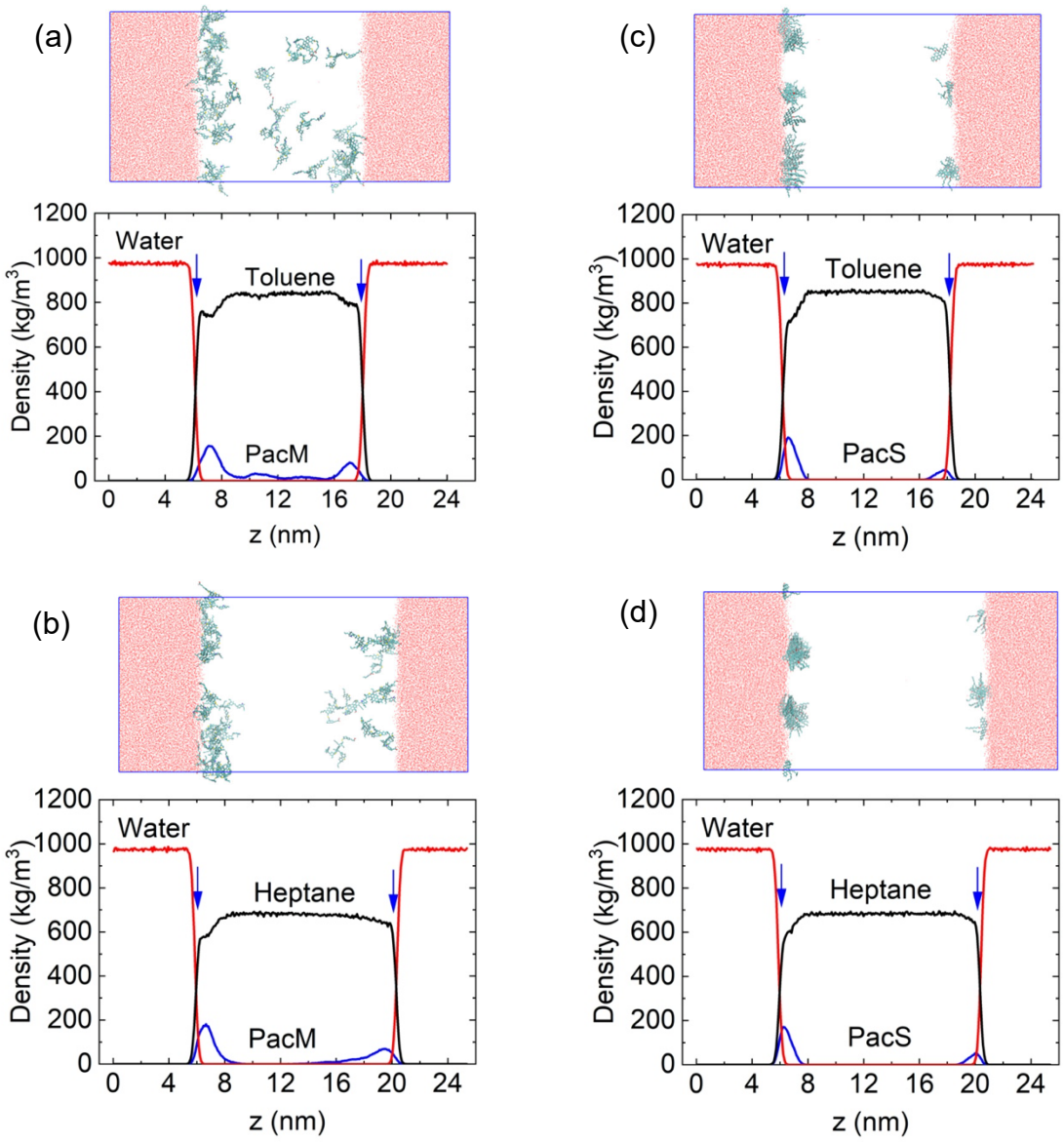

Figure 3. Density profiles of water, toluene or heptane, and PacM or PacS, averaged over the last 5 ns of the simulations for the control systems without non-ionic surfactants (a) sys. 1 (water/toluene with PacM); (b) sys. 6 (water/heptane with PacM); (c) sys. 11 (water/toluene with PacS); (d) sys. 16 (water/heptane with PacS). Above each subfigure is the snapshot of final configuration for the corresponding system (water molecules shown in red; heptane or toluene molecules removed for clarity; PacM or PacS molecules shown in cyan).

The number of adsorbed PAC molecules was quantified by the criterion that the minimum distance between PAC and the water phase was below 0.35 nm, as explained in SI section SI3. For all systems involving PacM molecules (sys. 1 to 10), the number of adsorbed PacM were stable over the last 5 ns of the simulations (see SI section SI4) and the averages are plotted in Fig. 4 (one decimal of the average value was kept). On the water/toluene interface, without non-ionic surfactants (sys. 1, shown as "None" in black symbol), the average number of adsorbed PacM molecules was 22.8. By adding NisB, the number of adsorbed PacM decreased to 18.2 at both low and high concentrations, indicating that the effect of NisB concentration was negligible. Adding NisP also resulted in a reduction of adsorbed PacM at water/toluene interface, but the effect of concentration was more significant. Lower concentration of NisP resulted in more desorption of the PacM, with 16.8 PacM remaining adsorbed as compared to 19.9 at high NisP concentration. On the water/heptane interface, as shown in Fig. 4 by red symbols, adding NisB reduced the number of adsorbed PacM molecules from 25.5 to 23.9 at lower concentration and to 23.6 at higher concentration. The difference caused by different NisB concentrations was again negligible. Interestingly, more PacM became adsorbed at the water/heptane interface with the addition of NisP, where lower concentration of NisP led to 26.2 adsorbed molecules and higher NisP concentration further increased the number to 28.5.

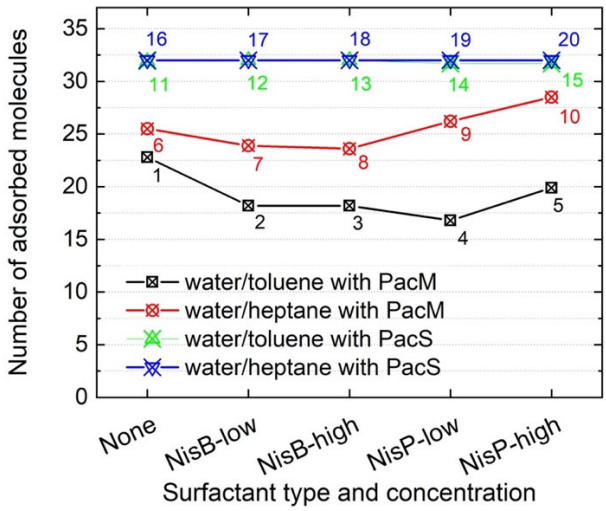

Figure 4. Number of adsorbed PAC molecules at organic solvent/water interface averaged over the last 5 ns of simulation. Water/toluene with PacM (black), water/heptane with PacM (red), water/toluene with PacS (green), water/heptane with PacS (blue). Horizontal labeling: (None) control systems without adding surfactants, sys. 1, 6, 11, 16; (NisB-low) adding NisB at low concentration, sys. 2, 7, 12, 17; (NisB-high) adding NisB at high concentration, sys. 3, 8, 13, 18; (NisP-low) adding NisP at low concentration, sys. 4, 9, 14, 19; (NisP-high) adding NisP at high concentration, sys. 5, 10, 15, 20. System number shown beside each symbol.

3.2 Role of non-ionic surfactants: competition vs. co-adsorption

The destabilization of water/oil interface by non-ionic surfactants have been frequently attributed to the competitive adsorption between non-ionic surfactants and PACs, where the non-ionic surfactants were more surface active and replaced the adsorbed PAC molecules [38,39,44,68,69]. Generally, if some adsorption sites were occupied by one component causing fewer adsorption sites available for other components, the situation was considered competitive adsorption. [70] In this work, competitive adsorption was identified if desorption of PACs was

observed along with simultaneous adsorption of non-ionic surfactants. On the other hand, the intermolecular interaction between non-ionic surfactants and PACs might assist their adsorption together on the interface, which represents co-adsorption [71].

The adsorptions of PACs and non-ionic surfactants were analyzed through their density distribution at equilibrium. Density profiles for PacM and NisB/P were averaged over the last 5 ns of simulation and plotted in Fig. 5a for sys. 2-5 (PacM in toluene) and Fig. 5b for sys. 7-10 (PacM in heptane). Two dashed lines in each system corresponded to the locations of interface-L and interface-R determined from the intersection of water and toluene (or heptane) density profiles. In each system, the curve for PacM or NisB/P had two peaks located near the interfaces, indicating the interfacial adsorption of both PacM and NisB/P. The black dot curve in each plot was the density profile of PacM in the corresponding control system, in absence of non-ionic surfactants. It should be noted that the locations of the two interfaces in systems with non-ionic surfactants were slightly different from the control systems, due to the change in box dimensions during the NpT simulation. In SI section SI5, the actual locations of the two interfaces in each system were given, along with locations of the peaks in the PacM density profiles. These data allowed us to calculate the distance between each PacM density peak and the nearest interface, as a measure of the proximity of PacM adsorption. By adding NisB at low concentration (sys. 2), the peak of PacM at interface-L was lowered but the peak at interface-R had no significant change. The curve for NisB had one peak on each interface, with zero values in bulk toluene, indicating their complete adsorption on the interfaces. Most of the NisB molecules were adsorbed at interface-L, where there was evident competitive adsorption between NisB and PacM. For sys. 3 with NisB at high concentration, the peak of PacM at interface-L was also lowered and both peaks shifted toward bulk toluene (see SI section SI5 for more details). Meanwhile, NisB showed two pronounced peaks

at the two interfaces. The adsorption of NisB also competed with the adsorption of PacM, pushing them towards the bulk. When NisP were added instead of NisB, sys. 4 and sys. 5 were found to behave similarly to sys. 3.

As shown in Fig. 5b, on the water/heptane interface, adding NisB at low concentration (sys. 7) did not have obvious effect on the peak of PacM near interface-L but slightly narrowed the peak near interface-R. The peaks of NisB at the two interfaces were weak and non-zero densities were found in bulk heptane, suggesting that the adsorption of NisB was incomplete. The adsorbed NisB competed with PacM, but the competition was very mild and only seen by the slight narrowing of the PacM peak at interface-R. Meanwhile, the dispersed NisB and PacM had interaction in bulk heptane, as shown in SI (section SI6). For sys. 8, the PacM peak at interface-L was lowered and shifted towards bulk heptane, while the peak at interface-R was narrowed but moved closer to the water phase (see SI section SI5 for more details). By adding NisP at low concentration (sys. 9), the changes in the PacM peaks were negligible. With NisP completely adsorbed at the interfaces, co-adsorption between NisP and PacM was observed. In sys. 10, the PacM peaks near both interfaces increased compared with the control system, signifying considerable co-adsorption of NisP and PacM.

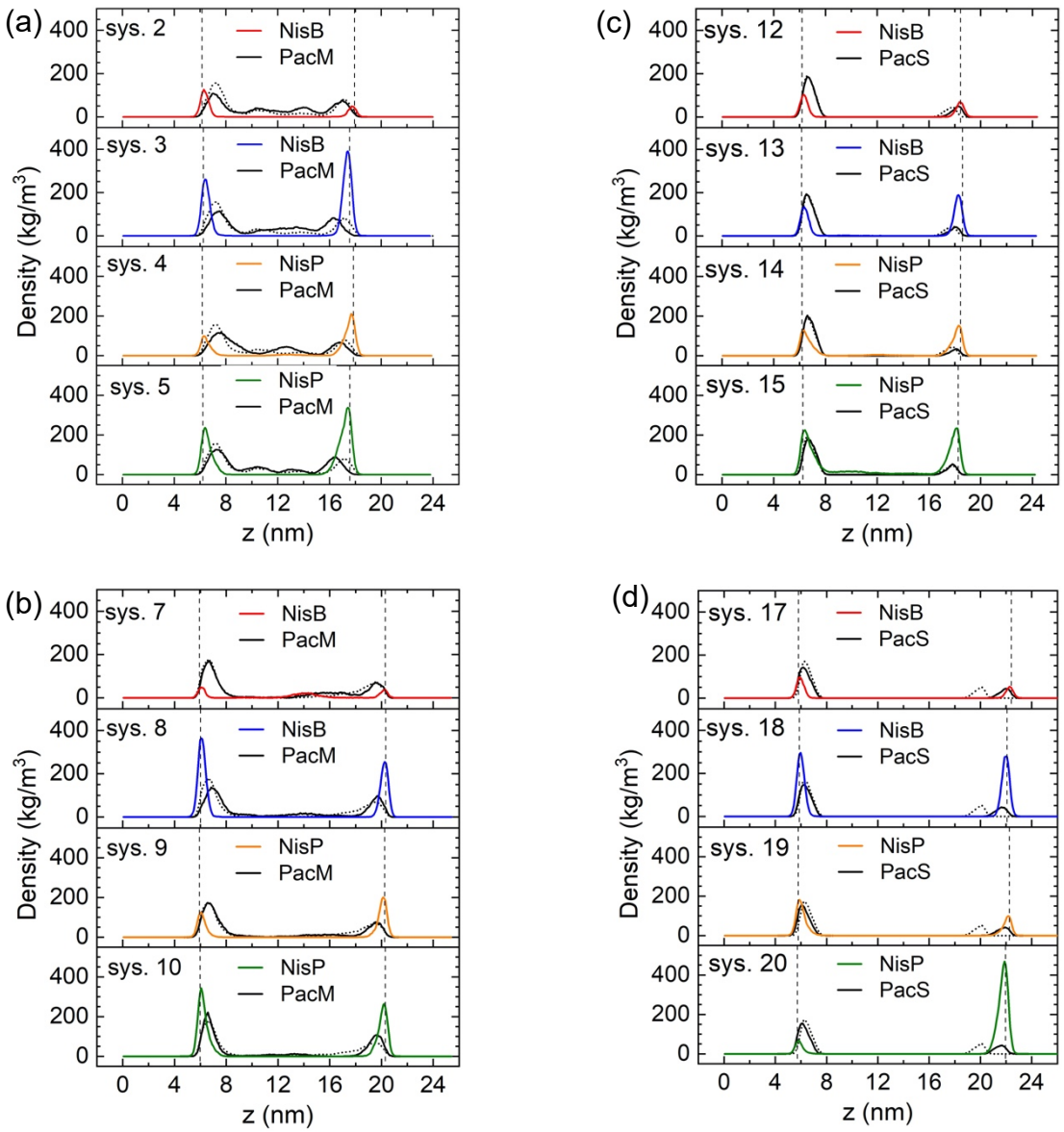

Figure 5. Density profiles for PacM/S and NisB/P averaged over last 5 ns for (a) sys. 2-5, PacM on water/toluene interface; (b) sys. 7-10, PacM on water/heptane interface; (c) sys. 12-15, PacS on water/toluene interface; and (d) sys. 17-20, PacS on water/heptane interface. In each plot, vertical dashed lines indicate the locations of the two interfaces, and the black dot curve is the density profile of PacM/S in the corresponding control systems.

The co-adsorption of PacM and NisB/P might be attributed to their intermolecular interactions, which was analyzed through the radial distribution function (RDF) of the atoms in NisB/P with

respect to the atoms in PacM, as plotted in Fig. 6a for sys. 2-5 (water/toluene interface) and in Fig. 6b for sys. 7-10 (water/heptane interface). RDF represents the probability of finding a particle at a certain radial distance from the reference particle, which is useful to identify interparticle structural correlations. [72] For example, de Oliveira et al. [73] simulated polyethylene glycol (PEG) polymers in water and chloroform solvents, and calculated the RDF between PEG groups in different polymers. The first peak in the RDF was located at 0.48 nm, corresponding to direct PEG-PEG interaction. The second peak was located at 0.59 nm, corresponding to PEG-PEG interaction mediated by solvent molecules. [73] The two non-ionic surfactants simulated in this work were not PEG but share some similarities at the end groups. On the other hand, the RDFs in Fig. 6 used the PAC atoms as the reference particles. The PACs do not have linear structures, and may not be able to interact with the surfactants at distances as close as those reported in de Oliveira et al. [73] In Fig. 6a, the first RDF peaks in sys. 2-5 (PacM in toluene) was located at 0.56 - 0.58 nm. The intensity of the first peak was quite low (around 1-2), indicating weak interaction between PacM and non-ionic surfactants. As shown in Fig. 6b, the first RDF peaks for sys. 7-10 were located at 0.54 - 0.56 nm, with low intensity (~ 3) for sys. 7-8 and higher intensity (~ 4.5-5.5) for sys. 9-10. The higher intensity for sys. 9-10 indicated a stronger correlation between PacM and NisP than between PacM and NisB in sys. 7-8. From the comparison of the first RDF peaks, the strength of short-range interaction between PacM and non-ionic surfactants was characterized as weak (intensity of peak: 1-2) in sys. 2-5, moderate (intensity of peak: 2-4) in sys. 7-8, and strong (intensity of peak over 4) in sys. 9-10. As mentioned in Fig. 5a-b, competitive adsorption was observed in sys. 2-5 and sys. 7-8, while co-adsorption was more dominant in sys. 9-10, which was correlated with the stronger interaction between PacM and non-ionic surfactants in sys. 9-10.

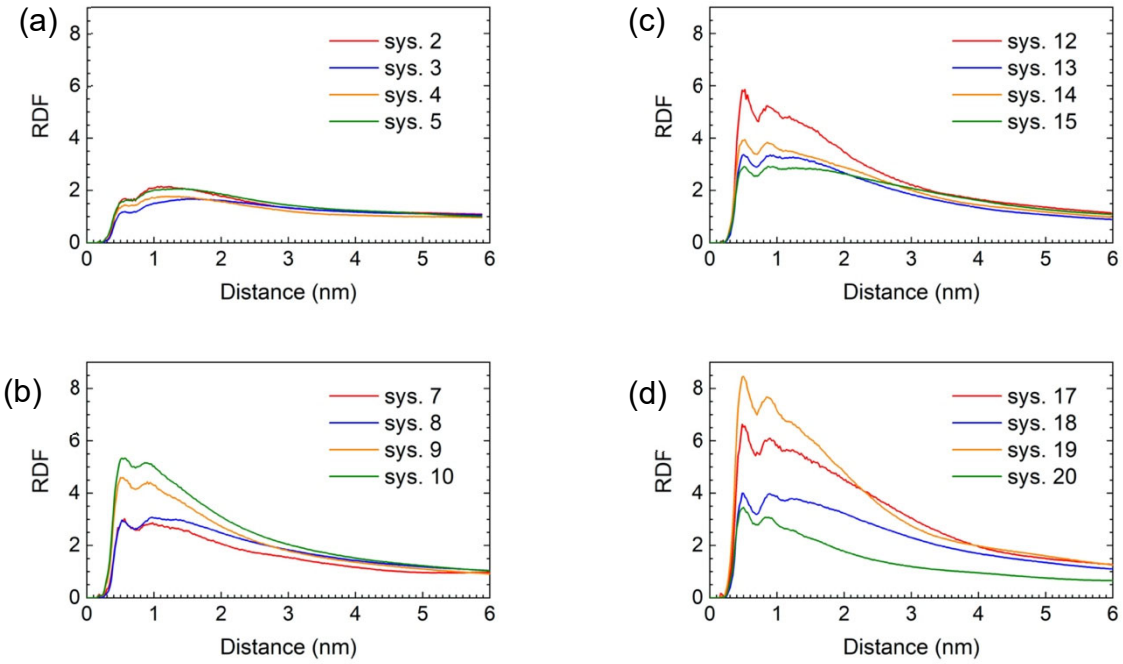

Figure 6. Radial distribution functions (RDFs) of all atoms in NisB/P molecules with respect to all atoms in PacM/S molecules, averaged over the last 5 ns, for (a) sys. 2-5, PacM on water/toluene interface; (b) sys. 7-10 PacM, on water/heptane interface; (c) sys. 12-15, PacS on water/toluene interface; and (d) sys. 17-20, PacS on water/heptane interface.

3.3 Co-adsorption between PacS and non-ionic surfactants

For the control systems with PacS, the density profiles stayed zero in bulk toluene (Fig. 3c) and heptane (Fig. 3d), indicating that all molecules were completely adsorbed at the interface. By introducing non-ionic surfactants into the water/toluene systems (sys. 12-15), as shown in Fig. 4, the number of adsorbed PacS molecules had no obvious change. It was consistent with the observation in Fig. 5c that the density profiles for PacS in sys. 12-15 with non-ionic surfactants almost overlapped with the curve for the control system (sys. 11). There was even a slight shift of the PacS peaks towards bulk water at interface-R for sys. 12-14, and at interface-L for sys. 15 (see SI section SI5 for more details). As shown in Fig. 6c, the first RDF peaks for sys. 12-15 had

intensity of ~ 2.5-6.0, indicating that the interaction between PacS and NisB/P was moderate (sys. 13-15) to strong (sys. 12). At water/heptane interface (sys. 17-20), Fig. 5d shows considerable shift of the PacS peaks towards the water phase, however this was mainly due to the change in the simulation box (see SI section SI5 for details). Nevertheless, the interaction between PacS and NisB/P (Fig. 6c) was moderate (sys. 18, sys. 20) to strong (sys. 17, sys. 19), and co-adsorption of NisB/P with PacS was evident.

3.4 Discussion

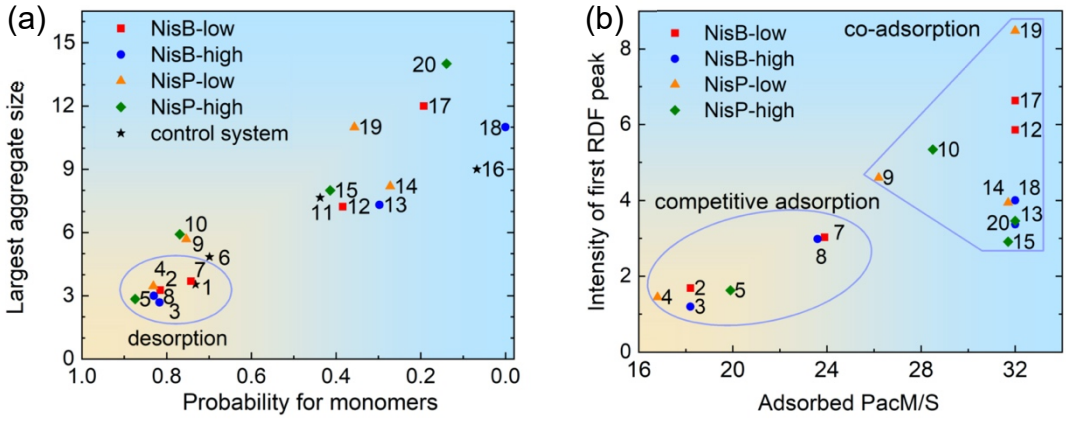

Figure 7. Summary of (a) the largest aggregate size vs. the probability of monomers; (b) the interaction between PacM/S and NisB/P vs. the number of adsorbed PacM/S molecules, where the interaction is represented by the intensity of the first RDF peaks in Fig. 6. Label on each symbol indicates the system number given in Table 1. All systems are mapped onto these two diagrams (control systems are excluded in (b)), based on data from the last 5 ns of the simulations.

Stable W-O emulsions were frequently attributed to the adsorption of PACs on the water/oil interface, which had certain correlation with the aggregation of PACs. [74–76] For example, Spiecker et al. [74] investigated the effect of resin on the aggregate size of PACs, and the stability

of W-O emulsion. With the increase of resin concentration, the aggregate size of PACs in mixtures of toluene and heptane, measured by small-angle neutron scattering, became smaller. [74] And the stability of W-O emulsion was lowered, due to the strong interaction between resin and PACs that interrupted the aggregation of PACs. [74] In our work, adding non-ionic surfactant also affect the aggregation of PACs. The aggregate size was quantified by the number of PAC molecules in the aggregate, which was determined by the criterion that any two PAC molecules in the aggregate had minimum distance less than 0.35 nm. The size of PAC aggregates was recorded over the last 5 ns of the simulations, and the probability distributions were plotted in SI section SI7. In addition, the size of the largest aggregates in each system was averaged over the last 5 ns of the simulations and reported in SI section SI8. Using the data from SI sections SI7 and 8, the aggregation of PAC molecules is compared in Fig. 7a through two aspects, the probability that PAC molecules existed as monomers (x axis) and the size of the largest aggregates (y axis). It was reported that compared with PacS, individual PacM molecules possessed intramolecular flexibility and could transition between folded and unfolded state in bulk toluene and heptane, which hindered aggregation [77]. As shown in Fig. 7a, PacM molecules also formed small aggregates (2-6 molecules in sys. 1-10), whereas PacS molecules formed larger aggregates (7-14 molecules in sys. 11-20). Also, compared with PacM for which the aggregates were loosely structured, the structure of PacS aggregates were more compact due to π–π stacking (see SI section SI9).

As Anton et al. [78] suggested, larger aggregates on the water/oil interface were more difficult to desorb than smaller aggregates. Among the systems containing PacM which formed smaller aggregates than PacS, desorption was observed in sys. 2-5 (PacM at water/toluene interface with NisB or NisP) and 7-8 (PacM at water/heptane interface with NisB), as marked in the blue circle in Fig. 7a. In these systems, the probability of monomers increased, and the size of the largest

aggregate decreased compared with the control systems, sys. 1 (PacM only on water/toluene interface) and sys. 6 (PacM only on water/heptane interface). This result implies the correlation between desorption and aggregation: desorption was more likely to occur upon the reduction of aggregate size and the increase of monomers, caused by adding non-ionic surfactants, as observed in sys. 2-5 and 7-8. In sys. 9-10, the largest aggregate size was increased by adding NisP on water/heptane interface, and desorption was not observed, which confirmed that larger aggregates were more difficult to desorb from the interface. It should be noted that all 32 PAC molecules were analyzed in Fig. 7a, and PAC monomers or the largest aggregates could be on the interface or dispersed in bulk organic phase. In fact, the largest aggregates were always observed on the interface except for sys. 2-3 where the largest aggregates were in bulk toluene. Large and compact aggregates formed by PacS were more difficult to desorb from the interface, and no desorption of PacS was observed for sys. 12-15 and 17-20 as shown in Fig. 7a.

Beside the effect of PAC structure, the aggregation and adsorption form of PAC at the interface also depended on the type of organic solvent. The PACs molecules had higher solubility in aromatic solvent (toluene) than in the aliphatic solvent (heptane). [59,77] Larger PAC aggregates could be formed in bulk heptane due to the solvent-solute incompatibility. [74] As shown in Fig. 7a, there were more PAC molecules in the largest aggregates on water/heptane interface. Also, more PacM molecules was adsorbed on the water/heptane interface than on water/toluene interface, which can be seen from Fig. 7b where the intensity of the first RDF peak from Fig. 6 is plotted against the number of adsorbed PAC molecules from Fig. 4. Mikami et al. [79] observed through MD simulations that their model single-core PACs had more adsorption on water/heptane interface than on water/toluene interface. The finding was similar to the case of PacM molecules in our work where there was more adsorption at water/heptane interface. In this work, PacS molecules were

completely adsorbed on both water/toluene and water/heptane interfaces, which was consistent with the simulation work from Lan et al. [59], but different from Mikami et al. [79]. One possible explanation is that the single core PAC model in Mikami's work had only one heteroatom, sulfur, located in the side chain, whereas the PacS molecule in our work had two oxygen atoms at the PA core, which could interact strongly with water phase and promote the adsorption of PacS molecules, as shown in SI section SI9.

The role of non-ionic surfactants is summarized in Fig. 7b. For sys. 2-3, and 7-8 marked in the blue circle, there was competitive adsorption between PacM and NisB. As discussed in Fig. 5a-b, all NisB were completely adsorbed in sys. 2, 3, and 8, while the adsorption of NisB in sys. 7 was incomplete due to their interaction with dispersed PacM in bulk heptane (SI section SI6). The adsorbed NisB molecules competed with PacM and caused desorption of PacM. Several factors contributed to the desorption of PacM by NisB. Firstly, NisB had hydrophilic ethyl oxide groups and chain-like structure with low molecular weight, which enabled the entire NisB molecule to be adsorbed close to the water phase, as shown in Fig. 5a-b and illustrated in SI section SI10. PacM molecules were larger and interacted with water mainly at the point of carboxyl group, while the rest of the molecule could be far from the water phase, as shown in SI section SI9 and SI10. With the adsorption of NisB, the interaction between PacM and water might be interrupted. Secondly, the interaction between NisB and PacM (Fig. 7b, y-axis) was weak for sys. 2-3 and moderate for sys. 7-8, thus the co-adsorption was insignificant. Thirdly, the adsorbed NisB interfered with the loosely structured PacM aggregates and promoted the dissociation of the aggregates into monomers. As discussed in Fig. 7a, the reduction of aggregate size and increase of monomers contributed to the desorption of PacM. It is important to mention that in our simulations, the concentration of NisB did not make significant difference in the desorption of PacM. On the

water/oil interface, the interfacial tension was governed by the surface concentration of PACs and not the bulk concentration, as pointed out by Jian et al. [41] In our work, while the bulk concentration of the solute was high (over 10,000 ppm) due to the small size of the simulation box, the maximum surface concentration possible was (32+128)/(2*144) = 0.56 molecules/nm^2, assuming all solutes were adsorbed. This concentration was less than half of the saturation surface concentration for single-core PAC on water/oil interface: 1.32 molecules/nm^2. [41] The insignificant effect of the concentration of non-ionic surfactants was likely caused by the fact that the interface was well below saturation.

The desorption of a mixture of PACs from water/xylene interface by adding Brij-93 were investigated by Pradilla et al. through interfacial tension measurement. [38,39] From Langmuir adsorption isotherm, they analyzed the composition on the interface and proposed the interaction between non-ionic surfactants and PACs. At low concentration of Brij-93 (10 ppm), there were interaction between Brij-93 and PACs and the partial desorption of PACs from the interface. [38] At higher concentration of Brij-93 (100 ppm), the PACs were almost completely desorbed from the interface and the interaction between Brij-93 and PACs diminished. [38] In our case, the interface with mixtures of PACs and NisB was below saturation, which corresponded to low concentration in the experiment. The low concentration scenario from Pradilla et al. [38] was consistent with our observation that there was weak (sys. 2-3) to moderate (sys. 7-8) interaction between Brij-93 (named NisB in this work) and PacM, and PacM molecules were partially desorbed from the interface. Other observation was obtained in this work for PacS molecules on water/toluene (sys. 12-13) and water/heptane (sys. 17-18) interfaces with the presence of NisB. The PacS molecules were difficult to desorb due to their large and compact aggregate structure, close contact with water phase, and moderate to strong interaction (Fig. 7b) with NisB.

In Pradilla et al.'s work [38,39], PE8100, a PEO-PPO copolymer, was shown to have better desorption capability than Brij-93, in that less amount of PE8100 was required to obtain similar degree of PAC desorption by Brij-93. At low concentration of PE8100 (0.5 ppm), strong interaction between PE8100 and PACs was observed and there was negligible desorption of PACs. [38,39] At high concentration of PE8100 (100 ppm), there was no interaction between PACs and PE8100, and PACs were completely desorbed. [38,39] The low concentration scenario in Pradilla et al.'s work was similar to sys. 9-10 in our work, where there was strong interaction between PacM and NisP, and co-adsorption was dominant on water/heptane interface, as shown in Fig. 7b. While for sys. 4-5 with PacM on water/toluene interface, the desorption of PacM by NisP could be attributed to the close contact between NisP and water phase, the small and loose structure of PacM aggregates, and the weak interaction between NisP and PacM. The effect of NisP concentration was more significant than NisB, probably due to the higher surface activity and molecular weight of NisP [38,39]. Increasing NisP concentration from sys. 4 to sys. 5, the desorption became less significant. And from sys. 9 to sys. 10, the co-adsorption of PacM and NisP was enhanced. The increased adsorption of PacM correlated with the increase of interaction between PacM and NisP (Fig. 7b). For systems with PacS (sys. 14-15, 19-20), co-adsorption between PacS and NisP was observed, similar to systems where NisB was added (sys. 12-13, 17-18).

In a previous simulation study, Niu et al. [44] placed a complete film of PEO-PPO copolymer and C5Pe, a model single-core PAC molecule, on water/xylene interface. They reported that the PEO-PPO copolymer could penetrate into and destroy the film formed by C5Pe. [44] Pradilla et al. [38,39] reported that with high concentration of non-ionic surfactants (2500 ppm of Brij-93 and 100 ppm of PE8100), the PACs could be completely displaced and there was no interaction

between PACs and non-ionic surfactant. Such complete desorption was not observed in our work, most likely due to the relatively low surface concentration of PACs and surfactants. While the bulk concentration of PACs can be assigned at the beginning of the simulations, their adsorption and hence surface coverage of the interface cannot be controlled. All of our simulations showed many of the PACs adsorbed in aggregated form, and even when they adsorbed in monomer form, their polyaromatic cores tended to be perpendicular or slant, instead of parallel, to the interface. Such configurations led to limited surface coverage of the interface, even though the bulk concentration was quite high. As shown in the SI (section SI11), the surface coverage fraction was 15% for sys. 1, 18% for sys. 6, and 11% for both sys. 11 and sys. 16. The surface coverage fraction was less than 20% in all cases, leave ample exposed interface where the non-ionic surfactants could adsorb and co-exist with the PACs. Although higher surface coverage was obtained for control systems with PacM than with PacS, the difference is small and the different desorption behaviors observed between PacM and PacS were mainly due to their different solubility, aggregation characteristics and interaction with the non-ionic surfactants. Our work shed light onto the different roles played by non-ionic surfactants on the adsorption of PAC on water/oil interface, which depend on PAC architecture, solvent and surfactant property. Competitive adsorption and desorption of the PACs may not be the only way to destabilize W-O emulsions; in fact, co-adsorption and subsequent bridging of small droplets have been proposed to be an alternative way of demulsification [59]. Understanding the roles of non-ionic surfactants is crucial to the design of chemical demulsifiers and control of their performance.

4. Conclusion

Molecular dynamics simulations were employed to investigate the adsorption of multi-core (PacM) and single-core (PacS) PACs at water/oil interfaces, in the presence of non-ionic surfactants (NisB and NisP). Different PAC architectures, solvent types, non-ionic surfactants and surfactant concentrations were used to investigate their influences. PacM tended to form smaller and more loosely structured aggregates at the interface, while the aggregates for PacS was larger and more compact. [77,79] There was more adsorption of PacM on water/heptane interface than on water/toluene interface, due to the lower solubility in heptane, whereas PacS molecules were completely adsorbed at both interfaces. [53,59,79,80]

NisB molecules were adsorbed closer to the water phase than PacM molecules due to the strong interaction between the hydrophilic EO group of NisB and water. The adsorbed NisB interfered with the interaction between PacM and water, as well as the interaction within the loosely structured PacM aggregates, causing them to dissociate into monomers that were easier to desorb [78]. For the surface concentrations obtained in this work, the bulk concentration of NisB did not have significant effect on the desorption of PacM, which was likely caused by the fact that the interface was well below saturation [41]. When NisP were added to the systems containing PacM and water/toluene interface, desorption was also observed. While on water/heptane interface, the interaction between NisP and PacM promoted the adsorption of PacM. The effect of NisP concentration was more significant than NisB, probably due to the higher surface activity and molecular weight of NisP [38,39], with the increase of NisP concentration favoring adsorption. Adding NisB or NisP did not induce the desorption of PacS, due to the large size and compact structure of PacS aggregates, the interaction between PacS and water, and the interactions between PacS and non-ionic surfactants.

This work identified two opposite roles of non-ionic surfactants on the adsorption of PACs, namely, competition and co-adsorption. While it was traditionally believed that competitive adsorption of non-ionic surfactants and their displacement of PACs were necessary for demulsification [44,81], our results showed that co-adsorption could also occur when there was a strong interaction between PACs and the surfactants. This phenomenon may not be detrimental to demulsification, and in fact suggests an alternative way of demulsification, by co-adsorption and subsequent bridging of small droplets into bigger ones which are then easier to be separated from the bulk phase [59]. To our best knowledge, this is the first atomistic-level study that comprehensively addressed the adsorption and interaction of PACs and non-ionic surfactants at water/oil interface under the influence of many important factors, such as PAC structure, solvent type, as well as structure and concentration of non-ionic surfactants. This work provided useful insights into the fundamental understanding of how non-ionic surfactants may modulate oil/water interfaces with adsorbed PACs, especially when they are used as chemical demulsifiers to treat water-in-oil emulsions. Future work will explore the coalescence or adhesion of water droplets with the presence of non-ionic surfactants, and a combined experimental and theoretical investigation on the stability of water-in-oil and oil-in-water emulsions with PACs and non-ionic surfactants.

Supporting information

Thermodynamic properties of model molecules; Equilibration of systems; Criterion for defining adsorbed PAC molecules; Number of adsorbed PacM molecules at the interface; Locations of interfaces and peaks in the PAC density profiles; Interaction between non-ionic surfactants and PacM in bulk organic phase; Probability distribution of aggregate size; Size of the largest

aggregates; Final configurations for control systems with top view on interface-L , and RDF between PACs; Final configurations for simulation sys. 2-5 and sys. 7-10; Fraction of surface coverage by PACs in control systems.

Acknowledgment

The authors gratefully acknowledge the computing resources and technical support from the Western Canada Research Grid (WestGrid), and the financial support from the Natural Sciences and Engineering Research Council of Canada (NSERC) and the Future Energy Systems under the Canada First Research Excellence Fund. The authors also thank Nexen Energy ULC for suggesting the molecular structure of the archipelago type model asphaltene, and Dr. Tu Lan for helpful discussions.

References

[1] A.G. Volkov, Liquid interfaces in chemical, biological and pharmaceutical applications, CRC Press, 2001.

[2] N. Somekawa, A. Yamauchi, K. Eda, T. Osakai, Computational Prediction of Adsorption Equilibrium for Nonionic Surfactants at the Oil/Water Interface, Langmuir. 35 (2019) 11345–11350. https://doi.org/10.1021/acs.langmuir.9b02193.

[3] D. Lavabre, V. Pradines, J.-C. Micheau, V. Pimienta, Periodic Marangoni Instability in Surfactant (CTAB) Liquid/Liquid Mass Transfer, J. Phys. Chem. B. 109 (2005) 7582–7586. https://doi.org/10.1021/jp045197m.

[4] N. Paul, P. Schrader, S. Enders, M. Kraume, Effects of phase behaviour on mass transfer in micellar liquid/liquid systems, Chem. Eng. Sci. 115 (2014) 148–156. https://doi.org/10.1016/j.ces.2013.02.018.

[5] M.A. Fulazzaky, Determining the resistance of mass transfer for adsorption of the surfactants onto granular activated carbons from hydrodynamic column, Chem. Eng. J. 166 (2011) 832–840. https://doi.org/10.1016/j.cej.2010.11.052.

[6] A. Wu, F. Lu, P. Sun, X. Gao, L. Shi, L. Zheng, Photoresponsive Self-Assembly of Surface Active Ionic Liquid, Langmuir. 32 (2016) 8163–8170. https://doi.org/10.1021/acs.langmuir.6b01937.

[7] J. Penfold, R.K. Thomas, H.-H. Shen, Adsorption and self-assembly of biosurfactants studied by neutron reflectivity and small angle neutron scattering: glycolipids, lipopeptides and proteins, Soft Matter. 8 (2012) 578–591. https://doi.org/10.1039/C1SM06304A.

[8] B. Dong, N. Li, L. Zheng, L. Yu, T. Inoue, Surface Adsorption and Micelle Formation of Surface Active Ionic Liquids in Aqueous Solution, Langmuir. 23 (2007) 4178–4182. https://doi.org/10.1021/la0633029.

[9] J.P. Rane, V. Pauchard, A. Couzis, S. Banerjee, Interfacial Rheology of Asphaltenes at Oil–Water Interfaces and Interpretation of the Equation of State, Langmuir. 29 (2013) 4750–4759. https://doi.org/10.1021/la304873n.

[10] A. Sarkar, D.S. Horne, H. Singh, Interactions of milk protein-stabilized oil-in-water emulsions with bile salts in a simulated upper intestinal model, Food Hydrocoll. 24 (2010) 142–151. https://doi.org/10.1016/j.foodhyd.2009.08.012.

[11] C. Shi, L. Zhang, L. Xie, X. Lu, Q. Liu, C.A. Mantilla, F.G.A. van den Berg, H. Zeng, Interaction Mechanism of Oil-in-Water Emulsions with Asphaltenes Determined Using Droplet Probe AFM, Langmuir. 32 (2016) 2302–2310. https://doi.org/10.1021/acs.langmuir.5b04392.

[12] C.-C. Chang, I. Williams, A. Nowbahar, V. Mansard, J. Mecca, K.A. Whitaker, A.K. Schmitt, C.J. Tucker, T.H. Kalantar, T.-C. Kuo, T.M. Squires, Effect of Ethylcellulose on the Rheology and Mechanical Heterogeneity of Asphaltene Films at the Oil–Water Interface, Langmuir. 35 (2019) 9374–9381. https://doi.org/10.1021/acs.langmuir.9b00834.

[13] H. Katepalli, A. Bose, T.A. Hatton, D. Blankschtein, Destabilization of Oil-in-Water Emulsions Stabilized by Non-ionic Surfactants: Effect of Particle Hydrophilicity, Langmuir. 32 (2016) 10694–10698. https://doi.org/10.1021/acs.langmuir.6b03289.

[14] B. Khadem, N. Sheibat-Othman, Modeling of double emulsions using population balance equations, Chem. Eng. J. 366 (2019) 587–597. https://doi.org/10.1016/j.cej.2019.02.092.

[15] C. Shi, L. Zhang, L. Xie, X. Lu, Q. Liu, J. He, C.A. Mantilla, F.G.A. Van den berg, H. Zeng, Surface Interaction of Water-in-Oil Emulsion Droplets with Interfacially Active

Asphaltenes, Langmuir. 33 (2017) 1265–1274. https://doi.org/10.1021/acs.langmuir.6b04265.
[16] L. Zhang, L. Xie, X. Cui, J. Chen, H. Zeng, Intermolecular and surface forces at solid/oil/water/gas interfaces in petroleum production, J. Colloid Interface Sci. 537 (2019) 505–519. https://doi.org/10.1016/j.jcis.2018.11.052.
[17] L. Xie, C. Shi, X. Cui, H. Zeng, Surface Forces and Interaction Mechanisms of Emulsion Drops and Gas Bubbles in Complex Fluids, Langmuir. 33 (2017) 3911–3925. https://doi.org/10.1021/acs.langmuir.6b04669.
[18] W. Zhou, L. Zhu, Distribution of polycyclic aromatic hydrocarbons in soil–water system containing a nonionic surfactant, Chemosphere. 60 (2005) 1237–1245. https://doi.org/10.1016/j.chemosphere.2005.02.058.
[19] X. Li, M. Yoneda, Y. Shimada, Y. Matsui, Effect of surfactants on the aggregation and stability of TiO2 nanomaterial in environmental aqueous matrices, Sci. Total Environ. 574 (2017) 176–182. https://doi.org/10.1016/j.scitotenv.2016.09.065.
[20] J. Long, L. Li, Y. Jin, H. Sun, Y. Zheng, S. Tian, Synergistic solubilization of polycyclic aromatic hydrocarbons by mixed micelles composed of a photoresponsive surfactant and a conventional non-ionic surfactant, Sep. Purif. Technol. 160 (2016) 11–17. https://doi.org/10.1016/j.seppur.2016.01.010.
[21] Z. Zheng, J.P. Obbard, Effect of non-ionic surfactants on elimination of polycyclic aromatic hydrocarbons (PAHs) in soil-slurry by Phanerochaete chrysosporium, J. Chem. Technol. Biotechnol. 76 (2001) 423–429. https://doi.org/10.1002/jctb.396.
[22] S.Y. Yuan, S.H. Wei, B.V. Chang, Biodegradation of polycyclic aromatic hydrocarbons by a mixed culture, Chemosphere. 41 (2000) 1463–1468. https://doi.org/10.1016/S0045-6535(99)00522-6.
[23] X. Zhu, G. Wu, D. Chen, Molecular Dynamics Simulation of Cyclodextrin Aggregation and Extraction of Anthracene from Non-Aqueous Liquid Phase, J. Hazard. Mater. 320 (2016) 169–175. https://doi.org/10.1016/j.jhazmat.2016.08.015.
[24] P. Tchoukov, F. Yang, Z. Xu, T. Dabros, J. Czarnecki, J. Sjöblom, Role of Asphaltenes in Stabilizing Thin Liquid Emulsion Films, Langmuir. 30 (2014) 3024–3033. https://doi.org/10.1021/la404825g.
[25] D.M. Sztukowski, M. Jafari, H. Alboudwarej, H.W. Yarranton, Asphaltene self-association and water-in-hydrocarbon emulsions, J. Colloid Interface Sci. 265 (2003) 179–186. https://doi.org/10.1016/S0021-9797(03)00189-9.
[26] S. Zhang, L. Zhang, X. Lu, C. Shi, T. Tang, X. Wang, Q. Huang, H. Zeng, Adsorption kinetics of asphaltenes at oil/water interface: Effects of concentration and temperature, Fuel. 212 (2018) 387–394. https://doi.org/10.1016/j.fuel.2017.10.051.
[27] D. Wang, Z. Zhao, C. Qiao, W. Yang, Y. Huang, P. McKay, D. Yang, Q. Liu, H. Zeng, Techniques for treating slop oil in oil and gas industry: A short review, Fuel. 279 (2020) 118482. https://doi.org/10.1016/j.fuel.2020.118482.
[28] X. Zhu, D. Chen, G. Wu, Molecular Dynamic Simulation of Asphaltene Co-Aggregation with Humic Acid During Oil Spill, Chemosphere. 138 (2015) 412–421. https://doi.org/10.1016/j.chemosphere.2015.06.074.
[29] L.A. Bernardez, S. Ghoshal, Solubilization kinetics for polycyclic aromatic hydrocarbons transferring from a non-aqueous phase liquid to non-ionic surfactant solutions, J. Colloid Interface Sci. 320 (2008) 298–306. https://doi.org/10.1016/j.jcis.2007.12.035.

[30] Z. Grenoble, S. Trabelsi, Mechanisms, performance optimization and new developments in demulsification processes for oil and gas applications, Adv. Colloid Interface Sci. 260 (2018) 32–45. https://doi.org/10.1016/j.cis.2018.08.003.
[31] G. Gelardi, S. Mantellato, D. Marchon, M. Palacios, A.B. Eberhardt, R.J. Flatt, Chemistry of chemical admixtures, in: Sci. Technol. Concr. Admix., Elsevier, 2016: pp. 149–218. https://doi.org/10.1016/B978-0-08-100693-1.00009-6.
[32] A.O. Adilbekova, K.I. Omarova, A. Karakulova, K.B. Musabekov, Nonionic surfactants based on polyoxyalkylated copolymers used as demulsifying agents, Colloids Surf. Physicochem. Eng. Asp. 480 (2015) 433–438. https://doi.org/10.1016/j.colsurfa.2014.11.004.
[33] Z. Li, H. Geng, X. Wang, B. Jing, Y. Liu, Y. Tan, Noval tannic acid-based polyether as an effective demulsifier for water-in-aging crude oil emulsions, Chem. Eng. J. 354 (2018) 1110–1119. https://doi.org/10.1016/j.cej.2018.08.117.
[34] E.I. Hernández, L.V. Castro-Sotelo, J.R. Avendaño-Gómez, C.A. Flores, F. Alvarez-Ramírez, F. Vázquez, Synthesis, Characterization, and Evaluation of Petroleum Demulsifiers of Multibranched Block Copolymers, Energy Fuels. 30 (2016) 5363–5378. https://doi.org/10.1021/acs.energyfuels.6b00419.
[35] G. Cendejas, F. Arreguín, L.V. Castro, E.A. Flores, F. Vazquez, Demulsifying super-heavy crude oil with bifunctionalized block copolymers, Fuel. 103 (2013) 356–363. https://doi.org/10.1016/j.fuel.2012.08.029.
[36] Z. Zhang, G.Y. Xu, F. Wang, S.L. Dong, Y.M. Li, Characterization and demulsification of poly(ethylene oxide)–block–poly(propylene oxide)–block–poly(ethylene oxide) copolymers, J. Colloid Interface Sci. 277 (2004) 464–470. https://doi.org/10.1016/j.jcis.2004.04.035.
[37] V.F. Pacheco, L. Spinelli, E.F. Lucas, C.R.E. Mansur, Destabilization of Petroleum Emulsions: Evaluation of the Influence of the Solvent on Additives, Energy Fuels. 25 (2011) 1659–1666. https://doi.org/10.1021/ef101769e.
[38] D. Pradilla, S. Simon, J. Sjöblom, Mixed Interfaces of Asphaltenes and Model Demulsifiers, Part II: Study of Desorption Mechanisms at Liquid/Liquid Interfaces, Energy Fuels. 29 (2015) 5507–5518. https://doi.org/10.1021/acs.energyfuels.5b01302.
[39] D. Pradilla, S. Simon, J. Sjöblom, Mixed interfaces of asphaltenes and model demulsifiers part I: Adsorption and desorption of single components, Colloids Surf. Physicochem. Eng. Asp. 466 (2015) 45–56. https://doi.org/10.1016/j.colsurfa.2014.10.051.
[40] F. Gao, Z. Xu, G. Liu, S. Yuan, Molecular dynamics simulation: the behavior of asphaltene in crude oil and at the oil/water interface, Energy Fuels. 28 (2014) 7368–7376. https://doi.org/10.1021/ef5020428.
[41] C. Jian, M.R. Poopari, Q. Liu, N. Zerpa, H. Zeng, T. Tang, Reduction of Water/Oil Interfacial Tension by Model Asphaltenes: The Governing Role of Surface Concentration, J. Phys. Chem. B. 120 (2016) 5646–5654. https://doi.org/10.1021/acs.jpcb.6b03691.
[42] T. Kuznicki, J.H. Masliyah, S. Bhattacharjee, Aggregation and Partitioning of Model Asphaltenes at Toluene−Water Interfaces: Molecular Dynamics Simulations, Energy Fuels. 23 (2009) 5027–5035. https://doi.org/10.1021/ef9004576.
[43] S. Hezaveh, S. Samanta, G. Milano, D. Roccatano, Molecular dynamics simulation study of solvent effects on conformation and dynamics of polyethylene oxide and polypropylene oxide chains in water and in common organic solvents, J. Chem. Phys. 136 (2012) 124901. https://doi.org/10.1063/1.3694736.

[44] Z. Niu, X. Ma, R. Manica, T. Yue, Molecular Destabilization Mechanism of Asphaltene Model Compound C5Pe Interfacial Film by EO-PO Copolymer: Experiments and MD Simulation, J. Phys. Chem. C. 123 (2019) 10501–10508. https://doi.org/10.1021/acs.jpcc.9b02248.
[45] F. Shehzad, I.A. Hussein, M.S. Kamal, W. Ahmad, A.S. Sultan, M.S. Nasser, Polymeric Surfactants and Emerging Alternatives used in the Demulsification of Produced Water: A Review, Polym. Rev. 58 (2018) 63–101. https://doi.org/10.1080/15583724.2017.1340308.
[46] M. Tomšič, M. Bešter-Rogač, A. Jamnik, W. Kunz, D. Touraud, A. Bergmann, O. Glatter, Nonionic Surfactant Brij 35 in Water and in Various Simple Alcohols: Structural Investigations by Small-Angle X-ray Scattering and Dynamic Light Scattering, J. Phys. Chem. B. 108 (2004) 7021–7032. https://doi.org/10.1021/jp049941e.
[47] A.B. Andrews, A. McClelland, O. Korkeila, A. Demidov, A. Krummel, O.C. Mullins, Z. Chen, Molecular Orientation of Asphaltenes and PAH Model Compounds in Langmuir−Blodgett Films Using Sum Frequency Generation Spectroscopy, Langmuir. 27 (2011) 6049–6058. https://doi.org/10.1021/la200466b.
[48] D. Liu, C. Li, X. Zhang, F. Yang, G. Sun, B. Yao, H. Zhang, Polarity effects of asphaltene subfractions on the stability and interfacial properties of water-in-model oil emulsions, Fuel. 269 (2020) 117450. https://doi.org/10.1016/j.fuel.2020.117450.
[49] C. Shi, L. Zhang, L. Xie, X. Lu, Q. Liu, J. He, C.A. Mantilla, F.G.A. Van den berg, H. Zeng, Surface Interaction of Water-in-Oil Emulsion Droplets with Interfacially Active Asphaltenes, Langmuir. 33 (2017) 1265–1274. https://doi.org/10.1021/acs.langmuir.6b04265.
[50] J. Dufour, J.A. Calles, J. Marugán, R. Giménez-Aguirre, J.L. Peña, D. Merino-García, Influence of hydrocarbon distribution in crude oil and residues on asphaltene stability †, Energy Fuels. 24 (2010) 2281–2286. https://doi.org/10.1021/ef900934t.
[51] J.M. Sheremata, M.R. Gray, H.D. Dettman, W.C. McCaffrey, Quantitative Molecular Representation and Sequential Optimization of Athabasca Asphaltenes, Energy Fuels. 18 (2004) 1377–1384.
[52] C. Jian, T. Tang, S. Bhattacharjee, Probing the Effect of Side-Chain Length on the Aggregation of a Model Asphaltene Using Molecular Dynamics Simulations, Energy Fuels. 27 (2013) 2057–2067. https://doi.org/10.1021/ef400097h.
[53] C. Jian, T. Tang, Molecular Dynamics Simulations Reveal Inhomogeneity-Enhanced Stacking of Violanthrone-78-Based Polyaromatic Compounds in *n* -Heptane–Toluene Mixtures, J. Phys. Chem. B. 119 (2015) 8660–8668. https://doi.org/10.1021/acs.jpcb.5b04481.
[54] A.D. Becke, A new mixing of Hartree–Fock and local density-functional theories, J. Chem. Phys. 98 (1993) 1372–1377. https://doi.org/10.1063/1.464304.
[55] A.K. Malde, L. Zuo, M. Breeze, M. Stroet, D. Poger, P.C. Nair, C. Oostenbrink, A.E. Mark, An Automated Force Field Topology Builder (ATB) and Repository: Version 1.0, J. Chem. Theory Comput. 7 (2011) 4026–4037. https://doi.org/10.1021/ct200196m.
[56] L.D. Schuler, X. Daura, W.F. van Gunsteren, An improved GROMOS96 force field for aliphatic hydrocarbons in the condensed phase, J. Comput. Chem. 22 (2001) 1205–1218. https://doi.org/10.1002/jcc.1078.
[57] C.M. Breneman, K.B. Wiberg, Determining atom-centered monopoles from molecular electrostatic potentials. The need for high sampling density in formamide conformational analysis, J. Comput. Chem. 11 (1990) 361–373. https://doi.org/10.1002/jcc.540110311.

[58] M.J. Frisch, G.W. Trucks, H.B. Schlegel, G.E. Scuseria, M.A. Robb, J.R. Cheeseman, G. Scalmani, V. Barone, G.A. Petersson, H. Nakatsuji, X. Li, M. Caricato, A.V. Marenich, J. Bloino, B.G. Janesko, R. Gomperts, B. Mennucci, H.P. Hratchian, J.V. Ortiz, A.F. Izmaylov, J.L. Sonnenberg, Williams, F. Ding, F. Lipparini, F. Egidi, J. Goings, B. Peng, A. Petrone, T. Henderson, D. Ranasinghe, V.G. Zakrzewski, J. Gao, N. Rega, G. Zheng, W. Liang, M. Hada, M. Ehara, K. Toyota, R. Fukuda, J. Hasegawa, M. Ishida, T. Nakajima, Y. Honda, O. Kitao, H. Nakai, T. Vreven, K. Throssell, J.A. Montgomery Jr., J.E. Peralta, F. Ogliaro, M.J. Bearpark, J.J. Heyd, E.N. Brothers, K.N. Kudin, V.N. Staroverov, T.A. Keith, R. Kobayashi, J. Normand, K. Raghavachari, A.P. Rendell, J.C. Burant, S.S. Iyengar, J. Tomasi, M. Cossi, J.M. Millam, M. Klene, C. Adamo, R. Cammi, J.W. Ochterski, R.L. Martin, K. Morokuma, O. Farkas, J.B. Foresman, D.J. Fox, Gaussian 16 Rev. C.01, Wallingford, CT, 2016.

[59] T. Lan, H. Zeng, T. Tang, Molecular Dynamics Study on the Mechanism of Graphene Oxide to Destabilize Oil/Water Emulsion, J. Phys. Chem. C. 123 (2019) 22989–22999. https://doi.org/10.1021/acs.jpcc.9b05906.

[60] J. Zielkiewicz, Structural properties of water: Comparison of the SPC, SPCE, TIP4P, and TIP5P models of water, J. Chem. Phys. 123 (2005) 104501. https://doi.org/10.1063/1.2018637.

[61] T. Kuznicki, J.H. Masliyah, S. Bhattacharjee, Molecular Dynamics Study of Model Molecules Resembling Asphaltene-Like Structures in Aqueous Organic Solvent Systems, Energy Fuels. 22 (2008) 2379–2389. https://doi.org/10.1021/ef800057n.

[62] D.V.D. Spoel, E. Lindahl, B. Hess, G. Groenhof, A.E. Mark, H.J.C. Berendsen, GROMACS: Fast, flexible, and free, J. Comput. Chem. 26 (2005) 1701–1718. https://doi.org/10.1002/jcc.20291.

[63] E. Lindahl, B. Hess, D. van der Spoel, Gromacs 3.0: A Package for Molecular Simulation and Trajectory Analysis, J. Mol. Model. 7 (2001) 306–317. https://doi.org/10.1007/s008940100045.

[64] H.J.C. Berendsen, D. van der Spoel, R. van Drunen, Gromacs: A Message-Passing Parallel Molecular Dynamics Implementation, Comput. Phys. Commun. 91 (1995) 43–56. https://doi.org/10.1016/0010-4655(95)00042-E.

[65] C. Oostenbrink, A. Villa, A.E. Mark, W.F.V. Gunsteren, A Biomolecular Force Field Based on the Free Enthalpy of Hydration and Solvation: The Gromos Force-Field Parameter Sets 53a5 and 53a6, J. Comput. Chem. 25 (2004) 1656–1676. https://doi.org/10.1002/jcc.20090.

[66] B. Hess, P-LINCS: A Parallel Linear Constraint Solver for Molecular Simulation, J. Chem. Theory Comput. 4 (2008) 116–122. https://doi.org/10.1021/ct700200b.

[67] U. Essmann, L. Perera, M.L. Berkowitz, T. Darden, H. Lee, L.G. Pedersen, A Smooth Particle Mesh Ewald Method, J. Chem. Phys. 103 (1995) 8577–8593. https://doi.org/10.1063/1.470117.

[68] Z. Niu, T. Yue, X. He, R. Manica, Changing the Interface Between an Asphaltene Model Compound and Water by Addition of an EO–PO Demulsifier through Adsorption Competition or Adsorption Replacement, Energy Fuels. 33 (2019) 5035–5042. https://doi.org/10.1021/acs.energyfuels.9b00741.

[69] E. Pensini, D. Harbottle, F. Yang, P. Tchoukov, Z. Li, I. Kailey, J. Behles, J. Masliyah, Z. Xu, Demulsification Mechanism of Asphaltene-Stabilized Water-in-Oil Emulsions by a Polymeric Ethylene Oxide–Propylene Oxide Demulsifier, Energy Fuels. 28 (2014) 6760–6771. https://doi.org/10.1021/ef501387k.

[70] J.J. Sheng, Surfactant-Polymer Flooding, in: Mod. Chem. Enhanc. Oil Recovery, Elsevier, 2011: pp. 371–387. https://doi.org/10.1016/B978-1-85617-745-0.00009-7.
[71] S. Liu, Cooperative adsorption on solid surfaces, J. Colloid Interface Sci. 450 (2015) 224–238. https://doi.org/10.1016/j.jcis.2015.03.013.
[72] T. Aste, T. Di Matteo, Nanometric architectures: emergence of efficient non-crystalline atomic organization in nanostructures, in: Nanostructure Control Mater., Elsevier, 2006: pp. 32–56. https://doi.org/10.1533/9781845691189.32.
[73] O.V. de Oliveira, L.T. Costa, E.R. Leite, Molecular modeling of a polymer nanocomposite model in water and chloroform solvents, Comput. Theor. Chem. 1092 (2016) 52–56. https://doi.org/10.1016/j.comptc.2016.08.005.
[74] P.M. Spiecker, K.L. Gawrys, C.B. Trail, P.K. Kilpatrick, Effects of petroleum resins on asphaltene aggregation and water-in-oil emulsion formation, Colloids Surf. Physicochem. Eng. Asp. 220 (2003) 9–27. https://doi.org/10.1016/S0927-7757(03)00079-7.
[75] J.D. McLean, P.K. Kilpatrick, Effects of Asphaltene Aggregation in Model Heptane–Toluene Mixtures on Stability of Water-in-Oil Emulsions, J. Colloid Interface Sci. 196 (1997) 23–34. https://doi.org/10.1006/jcis.1997.5177.
[76] S. Simon, J. Jestin, T. Palermo, L. Barré, Relation between Solution and Interfacial Properties of Asphaltene Aggregates, Energy Fuels. 23 (2009) 306–313. https://doi.org/10.1021/ef800548b.
[77] X. Sun, H. Zeng, T. Tang, Molecular simulation of folding and aggregation of multi-core polycyclic aromatic compounds, J. Mol. Liq. 310 (2020) 113248. https://doi.org/10.1016/j.molliq.2020.113248.
[78] N. Anton, T.F. Vandamme, P. Bouriat, Dilatational rheology of a gel point network formed by nonionic soluble surfactants at the oil–water interface, Soft Matter. 9 (2013) 1310–1318. https://doi.org/10.1039/C2SM27161C.
[79] Y. Mikami, Y. Liang, T. Matsuoka, E.S. Boek, Molecular Dynamics Simulations of Asphaltenes at the Oil–Water Interface: From Nanoaggregation to Thin-Film Formation, Energy Fuels. 27 (2013) 1838–1845. https://doi.org/10.1021/ef301610q.
[80] Y. Aray, R. Hernández-Bravo, J.G. Parra, J. Rodríguez, D.S. Coll, Exploring the Structure–Solubility Relationship of Asphaltene Models in Toluene, Heptane, and Amphiphiles Using a Molecular Dynamic Atomistic Methodology, J. Phys. Chem. A. 115 (2011) 11495–11507. https://doi.org/10.1021/jp204319n.
[81] Z. Li, S. Yin, G. Tan, S. Zhao, Z. Shi, B. Jing, L. Zhai, Y. Tan, Synthesis and properties of novel branched polyether as demulsifiers for polymer flooding, Colloid Polym. Sci. 294 (2016) 1943–1958. https://doi.org/10.1007/s00396-016-3956-x.